Research Journal of Applied Sciences, Engineering and Technology 13(5): 375-385, 2016
DOI:10.19026/rjaset.13.2955
ISSN: 2040-7459; e-ISSN: 2040-7467

Submitted: February 21, 2016 Accepted: May 13, 2016 Published: September 05, 2016

Research Article

Transient Stability Enhancement of Wind Farms using Photovoltaic Solar Plant as STATCOM

Khaled Benyahia, Larbi Boumediene and Abdelkader Mezouar
Laboratory of Electro-Technical Engineering, Tahar Moulay University of Saida, Algeria

Abstract: The aim of this study is to investigate the improvement of the performances and transient stability of grid connected Squirrel Cage Induction Generator based on Wind Farm (SCIG-WF) by using a new coordinated control between Grid Side Converter (GSC) of the Doubly Fed Induction Generator (DFIG) and photovoltaic solar plant converter (PV-SPC) as STATCOM. Thereby, the reactive power required by the SCIG-WF can be supplied either by the DFIGs (during normal condition) and with the PV-STATCOM during grid disturbances. This control strategy can fulfill the grid codes requirement such low voltage ride through capability by ensuring a no uninterrupted operation of the wind farm. The proposed control scheme is simulated by means of MATLAB/Simulink platform, based on a detailed system model. Through the simulated results, we can conclude that the proposed control for PV-SPC to operate as STATCOM is validated and the performances of the system are improved during normal and transient conditions.

Keywords: Doubly-fed induction generator, low voltage ride through, power quality, squirrel cage induction generator, system stability, voltage regulation

INTRODUCTION

In order to solve the energy crisis in the future, there are trends toward renewable energy technologies due to their advantages such abundance, maintenance-free, as well as assisting to decrease dependence on petroleum products (Yao *et al*., 2013; Chakraborty *et al*., 2013; Sumathi *et al*., 2015). Among these renewable energies, wind energy is one of the most popular and promising renewable energy in many countries. Its installation capacity was estimated to be 10% of the world's total electricity by the year 2020 and is expected to be double or more by the year 2040 (Cardenas *et al*., 2013; Shao *et al*., 2013).

The Wind Energy Conversion System (WECS) can be either fixed speed or variable speed, it all depends on the type of generator and the power electronics system used (Grigsby, 2012). Recently, the variable speed wind farm with Doubly Fed Induction Generators (DFIGs) is the most preferred technology compared to fixed speed wind farm applications because it offers several benefits such as the ability to get maximum power for any angular wind speed, reduce mechanical stresses and possibility to control active and reactive power independently. Additionally, the DFIG can contribute to improving the Low Voltage Ride Through (LVRT) capability during grid disturbance, which is considered as the main challenge in the grid-connected wind farm (Baggu, 2009; Abad *et al*., 2011; Aziz *et al*., 2014).

However, the fixed speed wind farm based on Squirrel Cage Induction Generators (SCIGs) with a direct connection to the grid which is the one of the oldest wind power system i.e., before year 2000, is still applicable in many countries due to their simplicity, cheap construction, smaller size and not require devices to synchronization with the grid. Nevertheless, there are numerous drawbacks of this kind of generators. The main one is the loss of reactive power control. In fact, a large amount of reactive power is consumed by the SCIG-WF during its operations (in steady-state and during transient conditions) which lead to overload issues and the WF should be immediately tripped from the grid. Generally, external devices for reactive power compensation is equipped with this machine (Farret *et al*., 2014; Duong *et al*., 2015; Tan, 2016).

On the other hand, recent grid code standards like IEEE1547 and the order No. 661 published by Federal Energy Regulatory Commission (FERC) requires to the wind power system to stay connected to the grid during a fault in order to provide the low voltage ride through (LVRT) capability and to contribute to the voltage recovery (Baggu, 2009; Aziz *et al*., 2014).

Corresponding Author: Khaled Benyahia, Laboratory of Electro-Technical Engineering, Tahar Moulay University of Saida, Algeria, Tel.: 00213773801781

Hence, many works have been developed and numerous techniques have been proposed. For instance, the phase-controlled soft starter technique is used to limit the RMS values of the inrush currents to a level below two times of the SCIG rated current (Qiao, 2012). The capacitor banks are usually used with the SCIG to supply enough reactive power (Blaabjerg and Ma, 2014). Furthermore, the flexible alternating current transmission systems (FACTS) devices such as StaticVar Compensator (SVC) and STATCOM, can also be used to fulfill the grid codes requirements by solving the reactive power issues and voltage stability in the power system (Luo *et al*., 2016). As proposed in Suul *et al*. (2010) and Obando-Montaño *et al*. (2014), the STATCOM is used to control the bus voltage and enhance the LVRT of wind farm based SCIG during grid disturbance.

A performance comparison between the SVC and STATCOM to improve the stability of wind farm based SCIG is presented in Xu *et al*. (2006). In a recent study, a hybrid control technique based on proportional-integral (PI) controller and a fuzzy technique for pitch angle control are investigated to improve the power quality and transient stability of SCIG-WF (Duong *et al*., 2015).

However, these solutions are considered more expensive and uneconomically, which lead to increase the overall system cost.

Moreover, the STATCOM is based on the DC/AC converter, which has a similar converter structure to that used in grid-connected renewable energy conversion systems. So, it can be used as an STATCOM if an appropriate control is applied. As suggested in Bhaskar *et al*. (2012) and Varma *et al*. (2015), the photovoltaic solar plant converter (PV-SPC) is used as STATCOM, called PV-STATCOM to improve the interconnected transmission system stability and to regulate grid voltage.

This study extends the work of Varma *et al*. (2015) by proposing a new contribution which consists of introducing the DFIG wind farm and PV-STATCOM to improve the performances and the stability of the existing SCIG-WF and to ensure uninterrupted operations of the wind farm by controlling the PCC voltage. Thereby, if the converter of DFIG is not able to supply enough reactive power to the system during the grid disturbance, the PV-STATCOM can provide the required reactive power. In addition, the solar farm converter can operate as STATCOM in the day and in the night. At the day time, the PV-SPC provides power to grid in the normal operations. However, when there is a disturbance in the power system, the PV-SPC operates as STATCOM to regulate the voltage at PCC by using the inverter capacity left after real power generation. While at night time which is inactive, the DC capacitor is charged from the main grid and the total capacity rating of PV-SPC is used to perform the aforementioned operations. Hence, the efficiency and the performances of the SCIG-WF can be improved.

MATERIALS AND METHODS

System configuration: The structure of the system to be studied is shown in Fig. 1 which is composed of two wind farms, the first one which is the main wind farm included 4.5 MW SCIG wind turbines and the second consists of 4.5 MW DFIG wind turbines. The two wind farms are simulated by an aggregate model, i.e. the total of the turbines is modeled as one generator and are connected to the PCC distribution system through transformers. A 3-MVAr PV solar farm acts as STATCOM is also connected to the PCC.

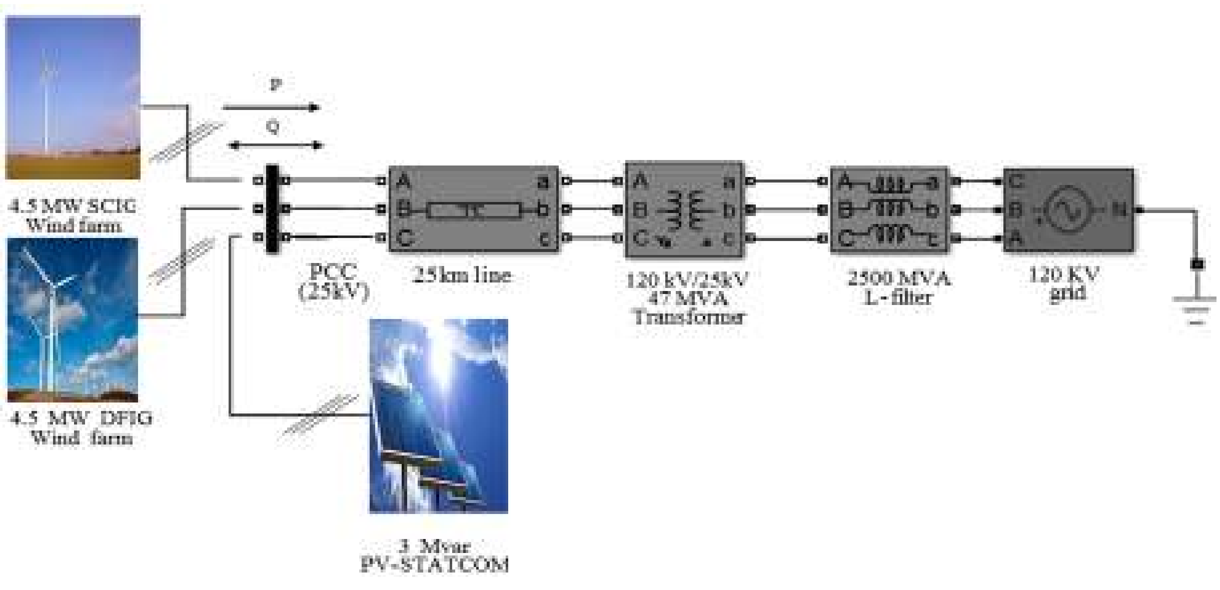

Fig. 1: Schematic diagram of system study

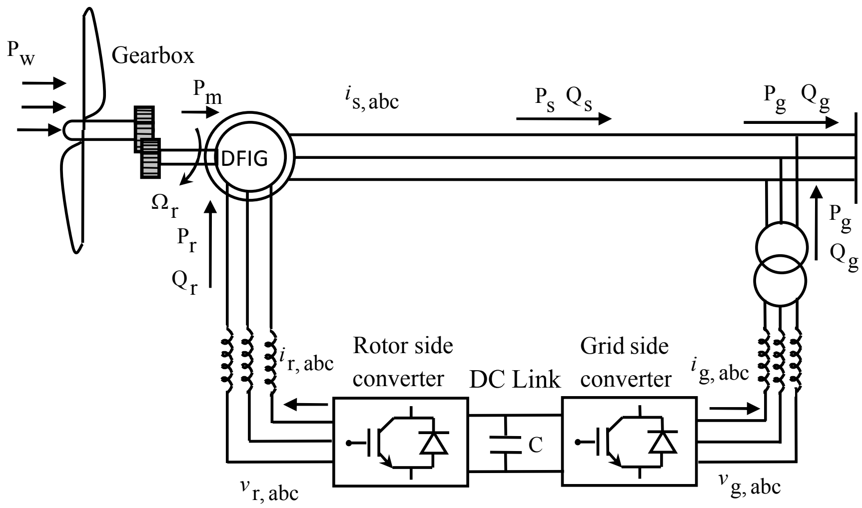

Fig. 2: Scheme of DFIG equipped wind turbine

A transformer and transmission line is used to connect the system with the grid.

System modeling and control:

DFIG model: The construction of the DFIG consists of a three phase stator winding connected directly to the grid and a three phase rotor winding connected also to the grid through a back-to-back converter with capacitor dc-link (AC/DC/AC) as shown in Fig. 2.

The mathematic model of the DFIG in Park reference frame can be expressed by the following equations (Abad *et al*., 2011; Zou *et al*., 2013; Farret *et al*., 2014):

Stator and rotor voltages:

$$\begin{cases} v_{ds} = R_s i_{ds} + \dfrac{d}{dt}\varphi_{ds} - \omega_s \varphi_{qs} \\ v_{qs} = R_s i_{qs} + \dfrac{d}{dt}\varphi_{qs} + \omega_s \varphi_{ds} \\ v_{dr} = R_r i_{dr} + \dfrac{d}{dt}\varphi_{dr} - (\omega_s - \omega_r)\varphi_{qr} \\ v_{qr} = R_r i_{qr} + \dfrac{d}{dt}\varphi_{qr} + (\omega_s - \omega_r)\varphi_{dr} \end{cases} \quad (1)$$

Flux- current relations are expressed as:

$$\begin{cases} \varphi_{ds} = L_s i_{ds} + M i_{dr} \\ \varphi_{qs} = L_s i_{qs} + M i_{qr} \\ \varphi_{dr} = L_r i_{dr} + M i_{ds} \\ \varphi_{qr} = L_r i_{qr} + M i_{qs} \end{cases} \quad (2)$$

The electromagnetic torque is given as:

$$T_{em} = p\frac{M}{L_s}(\varphi_{qs} i_{dr} - \varphi_{ds} i_{qr}) \quad (3)$$

The stator active and reactive powers of DFIG is given by:

$$\begin{cases} P_s = v_{ds} i_{ds} + v_{qs} i_{qs} \\ Q_s = v_{qs} i_{ds} - v_{ds} i_{qs} \end{cases} \quad (4)$$

where, R_s and R_r are, respectively, the stator and rotor phase resistances. L_s is stator inductance. M is mutual inductance. $\varphi_{ds}, \varphi_{qs}, \varphi_{dr}, \varphi_{qr}$ are respectively direct and quadrature stator flux and direct and quadrature rotor flux. i_{ds} , i_{qs} and i_{dr} , i_{qr} are, respectively the direct and quadrate stator and rotor currents. p is the pair of poles number. ω_s and ω_r are the angular speed of stator and rotor; respectively.

SCIG modelling: The structure of this generator in wind turbine consists of a stator winding which is connected directly to the grid as shown in Fig. 3.

The mathematic model of the SCIG in Park reference frame is the same model as the DFIG except in the rotor voltages which are set by zero as (Grigsby, 2012; Zou *et al*., 2013; Chakraborty *et al*., 2013):

$$\begin{cases} v_{ds} = R_s i_{ds} + \dfrac{d}{dt}\varphi_{ds} - \omega_s \varphi_{qs} \\ v_{qs} = R_s i_{qs} + \dfrac{d}{dt}\varphi_{qs} + \omega_s \varphi_{ds} \\ v_{dr} = 0 = R_r i_{dr} + \dfrac{d}{dt}\varphi_{dr} - \omega_r \varphi_{qr} \\ v_{qr} = 0 = R_r i_{qr} + \dfrac{d}{dt}\varphi_{qr} + \omega_r \varphi_{dr} \end{cases} \quad (5)$$

Control strategy of DFIG: Since the DFIG is connected to the utility grid, the power exchanged between this machine and the grid should be controlled independently both in magnitude and in the direction in order to produce electrical power at constant voltage and frequency. Hence, the back-to-back converter with

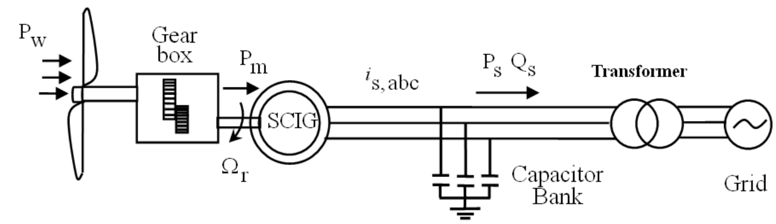

Fig. 3: Scheme of SCIG based wind turbine

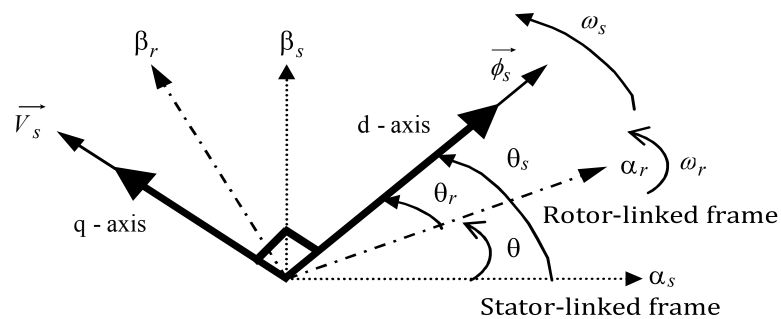

Fig. 4: Stator flux-oriented vector controls scheme for RSC

capacitor dc-link (AC/DC/AC) is used, which contains the Rotor Side Converter control (RSC) control and the Grid Side Converter control (GSC) control (Cardenas *et al*., 2013; Farret *et al*., 2014; Sumathi *et al*., 2015).

Rotor side converter control: The main function of the RSC of the DFIG is to control separately the stator active and reactive powers.

Hence, vector control technique with field oriented schemes is generally employed.

The Stator Flux Oriented reference frame (SFO) is the mostly used in DFIG, where the d-axis of the reference frame is aligned with the stator flux as shown in Fig. 4. Consequently, $\varphi_{ds} = \varphi_s$ and (Grigsby, 2012; Cardenas *et al*., 2013; Farret *et al*., 2014; Sumathi *et al*., 2015).

If the grid is assumed to be stable and stator resistance is neglected this is an assumption for a machine of large power, thus $\o_{ds}$ constant.
Rotor voltages can be expressed as:

$$\begin{cases} v_{dr} = \sigma L_r \dfrac{di_{dr}}{dt} + R_r i_{dr} - \sigma L_r \omega_r i_{qr} + \dfrac{M}{L_s}\dfrac{d\varphi_{ds}}{dt} \\ v_{qr} = \sigma L_r \dfrac{di_{qr}}{dt} + R_r i_{qr} + \sigma L_r \omega_r i_{dr} + s\dfrac{M}{L_s} Vs \end{cases} \tag{6}$$

Using this assumption, the stator active and reactive powers can be expressed as the function of rotor currents as:

$$\begin{cases} P_s = -V_s \cdot \dfrac{M}{L_s} i_{qr} \\ Q_s = -V_s \cdot \dfrac{M}{L_s}\left(i_{dr} - \dfrac{\varphi_{ds}}{M} \right) \end{cases} \tag{7}$$

From Eq. (7) it is obviously shown that the stator active power can be controlled by setting the quadrate rotor current and the reactive power can be regulated by means of the direct rotor current. The vector control scheme of the RSC is depicted in Fig. 5.

Grid Side Converter control (GSC): The main function of the GSC is to regulate the DC link voltage and keeps it at a constant value.

Therefore, the GSC can be designed to control the reactive power exchanged with the grid. Similar vector control approach that applied in the RSC is used for the GSC to control independently the active and reactive power followed between the grid and the converter.

This control scheme is based on current regulation, with the d-axis current regulates the dc-link voltage, while the q-axis current controls the reactive power. The overall vector control scheme for the grid-side converter is shown in Fig. 6.

Due to the small capacity rating of power converters of the DFIG, typically about 25 to 30% of the total power rating, the capability to provide reactive power is limited that an external device is needed to ensure stable operation (Grigsby, 2012; Cardenas *et al*., 2013; Farret *et al*., 2014; Sumathi *et al*., 2015).

Photovoltaic solar energy: The concept of photovoltaic energy is to convert the sunlight directly into electricity through the photovoltaic cells (Sumathi *et al*., 2015).

To achieve the required current and voltage, photovoltaic cells are combined in series and parallel to form a module and to attain the desired power, several modules are connected together to form an array as

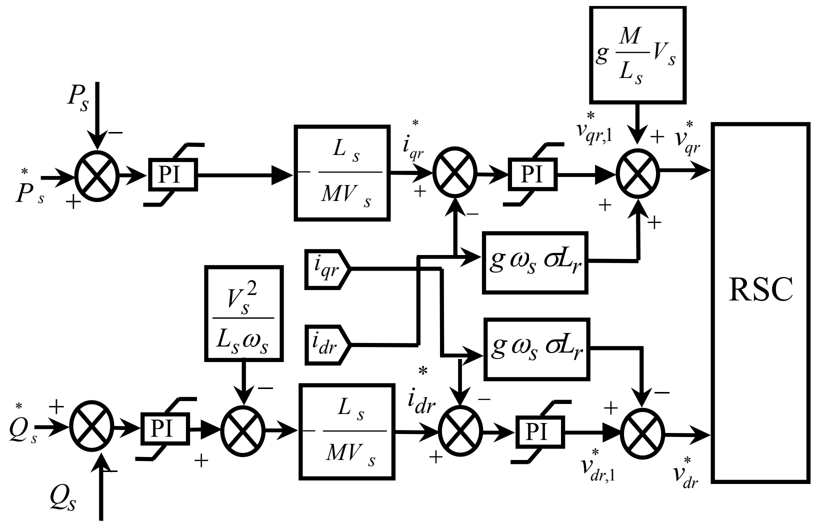

Fig. 5: Vector control scheme for the RSC

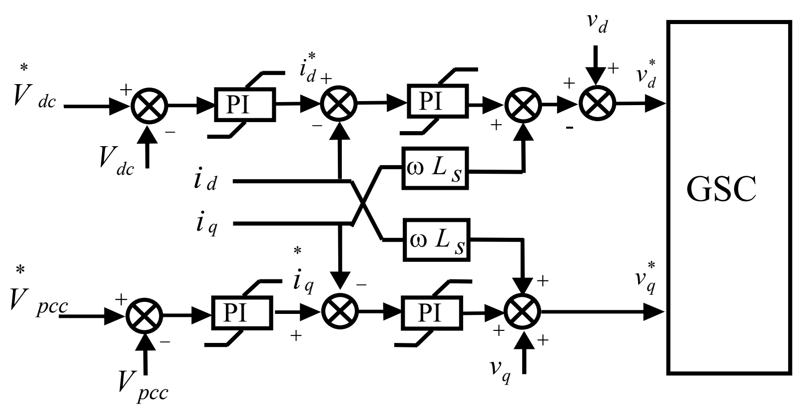

Fig. 6: Control scheme for the GSC

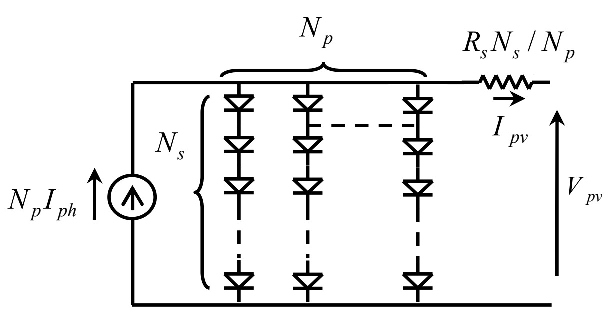

Fig. 7: Electrical circuit of solar PV array

shown in Fig. 7 (Abdul Rauf *et al*., 2015; Sumathi *et al*., 2015).

The curves of current voltage I-V and power voltage P-V characteristics for one module which constituting of 96 cells of Sun-Power (SPR-305) for solar irradiation are shown in Fig. 8.

Electrical characteristic in Table 1 (Gupta *et al*., 2014). As we can see, the PV module presents a nonlinearity feature in the P-V curves when the solar irradiation and changes. Moreover, there is only one point on the curves, termed Maximum Power Point (MPP) at which the generated power is maximum. Therefore, Maximum Power Point Tracking (MPPT) techniques is needed in PV system to ensure that the PV array always generates maximum power for any given of temperature and solar insolation (Muthuramalingam and Manoharan, 2014; Sankarganesh and Thangavel, 2014).

Table 1: Electrical characteristic of one solar PV-module (S.P.R-305-WHT) (Gupta *et al*., 2014)

Parameter	Variable	Value
Power rating at Standard Test Conditions (STC)	Pmp	305 W
Open-circuit voltage	Voc	64.2 V
Voltage at maximum power	Vmp	54.7 V
Current at maximum power	Imp	5.58 A
Short circuit current	Isc	5.96 A
Number of cells per module	Ns	96

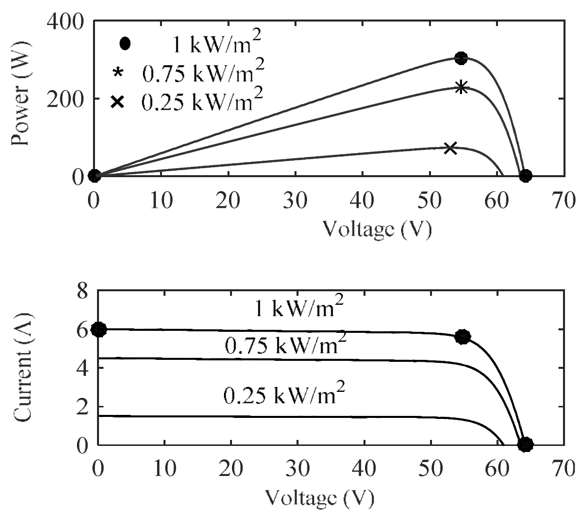

Fig. 8: PV-module characteristics for different solar irradiation

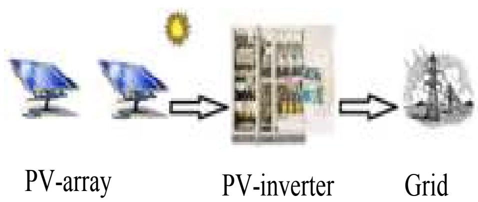

Fig. 9: Schematic diagram of grid-connected PV system

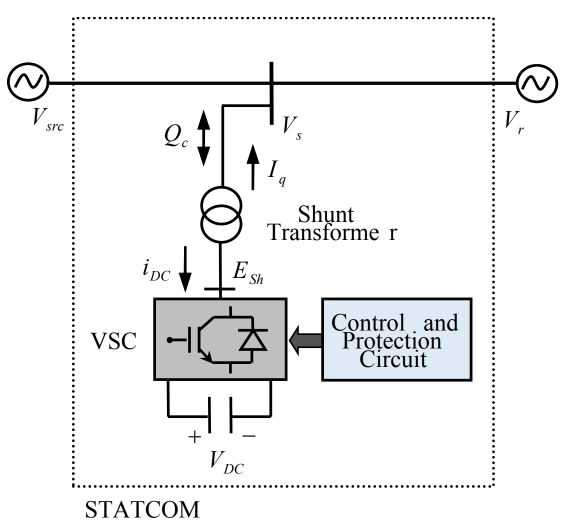

Fig. 10: The basic model of STATCOM

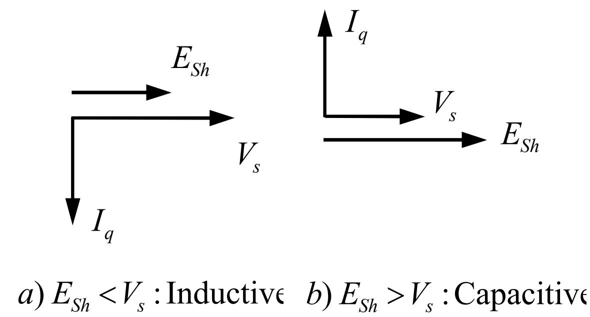

Fig. 11: STATCOM operation modes

The photovoltaic solar energy can be classified into grid connected and stand- alone systems.

In the grid-connected system, the DC /AC power converter is required to convert DC power to AC power at desired output voltage and frequency (Malek, 2014; Bhatti *et al*., 2015; Sumathi *et al*., 2015).

Figure 9 shows the basic components of grid-connected PV system.

STATCOM: The static synchronous compensator (STATCOM) also known as advanced SVC is a power electronic component from the FACTS family devices, it connected in shunt with power grid system for voltage regulation purpose and for reactive power compensation (Sen and Sen, 2009; Luo *et al*., 2016). The main components of STATCOM is a VSC which generally based on IGBT or GTO self-commutated power semiconductor with a DC link capacitor, a shunt transformer and a control circuit, as shown in Fig. 10.

In order to regulate the system voltage, the STATCOM injects a sinusoidal reactive current *Iq* of variable magnitude to the compensating system through a reactance. The magnitude and the direction of this current depend on the STATCOM voltage magnitude which is in phase with the line voltage.

When the line voltage is higher than the STATCOM voltage the current *Iq* injected to the transmission line is lags the line voltage by 90° as shown in Fig. 11a and the STATCOM acts as an inductor (inductive mode). The reactive power is then absorbed from the transmission line. Whereas, when the line voltage is lower than the STATCOM voltage the current *Iq* injected to the transmission line leads the line voltage by 90° as shown in Fig. 11b and the STATCOM operates as a capacitor (capacitive mode) and the reactive power is injected into the transmission line (Sen and Sen, 2009).

The STATCOM has numerous advantage over the traditional reactive power compensation such SVC and synchronous condenser is characterized by a fast response and provide a smooth reactive power (Padiyar, 2007; Sen and Sen, 2009; Luo *et al*., 2016).

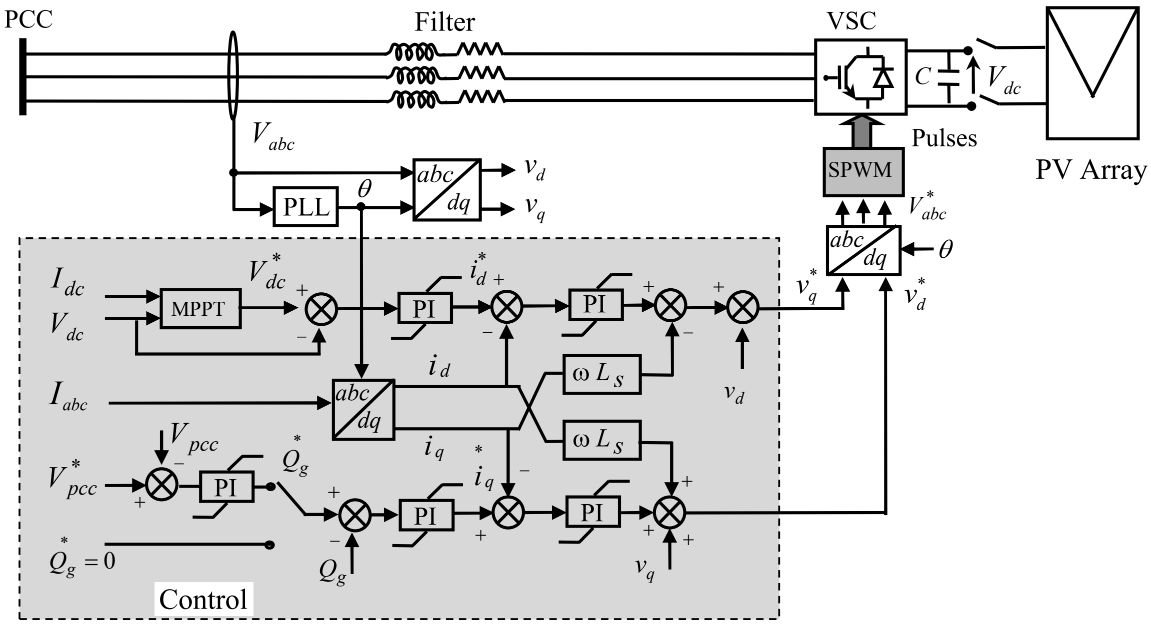

Fig. 12: Control scheme of PVSP converter

Control structure of PV inverter: In order to make the PV-inverter operates as STATCOM, a control technique is proposed as shown in Fig. 12. This control strategy consists of two cascade control loops, the first loop is used to regulate the DC link voltage and maintain it at a constant value.

Whilst, the second loop control the voltage and the reactive power at PCC.

In normal conditions, the reference value of reactive power is set by zero $Q_{ref} = 0$ in order to keep unity power factor and when the grid fault occurs, the PV plant is disconnected from the main network via a protection system to avoid islanding phenomena and now the control of reactive power changes to voltage regulation. The switching signals for the PV-SPC are generated by using the Sinusoidal Pulse Width Modulation Technique (SPWM). The phase-locked loop (PLL) is used to synchronize the converter with the grid.

Table 2: Wind farm induction generators parameters

	Induction generators parameters	
Variable	DFIG	SCIG
Rated power	4.5 MW	4.5 MW
Rated voltage	575 V	575 V
Stator resistance	0.00706 pu	0.00706 pu
Rotor resistance	0.005 pu	/
Mutual Inductance	2.9 pu	/

Table 3: Parameters of photovoltaic solar farm and converter

Variable	Photovoltaic system parameters Solar farm
Nominal Active Power of PV SP	1.5 MW
Number of series-parallel connected modules	4 884
Photovoltaic solar farm converter parameters	
Rated power	3 MVar
Rated voltage	25000 V
DC link voltage	4000 V
DC link capacitance	11 000 μF
PCC voltage regulator gains Kp and Ki	[5-1000]

RESULTS AND DISCUSSION

In this section, the simulation studies of the proposed system are carried out on the MATLAB/Simulink platform and the results are presented and discussed.

The system parameters are listed in the Table 2 and 3. In order to show the efficiency of the proposed system, three cases studies are simulated: Firstly, the wind farm with the SCIG is tested alone without any compensation to show its behavior. Secondly, the DFIG wind farm is introduced in the PCC when the SCIG-WF is connected.

In the third scenario, the whole system equipped with PV-STATCOM is tested under a fault condition, which is represented by a dip voltage in the grid side in order to prove the performance against grid disturbance.

The operation of the system without any compensation is depicted in Fig. 13. The fluctuations presented in the results from t = 0 s to t = 2.5 s. are due to the initial conditions. As we can see, the voltage at PCC is below than its rated value 1 p.u. This phenomena is due to the lack of reactive power support which consumed to magnetize the machine, as discussed in Qiao (2012) and Sumathi *et al*. (2015).

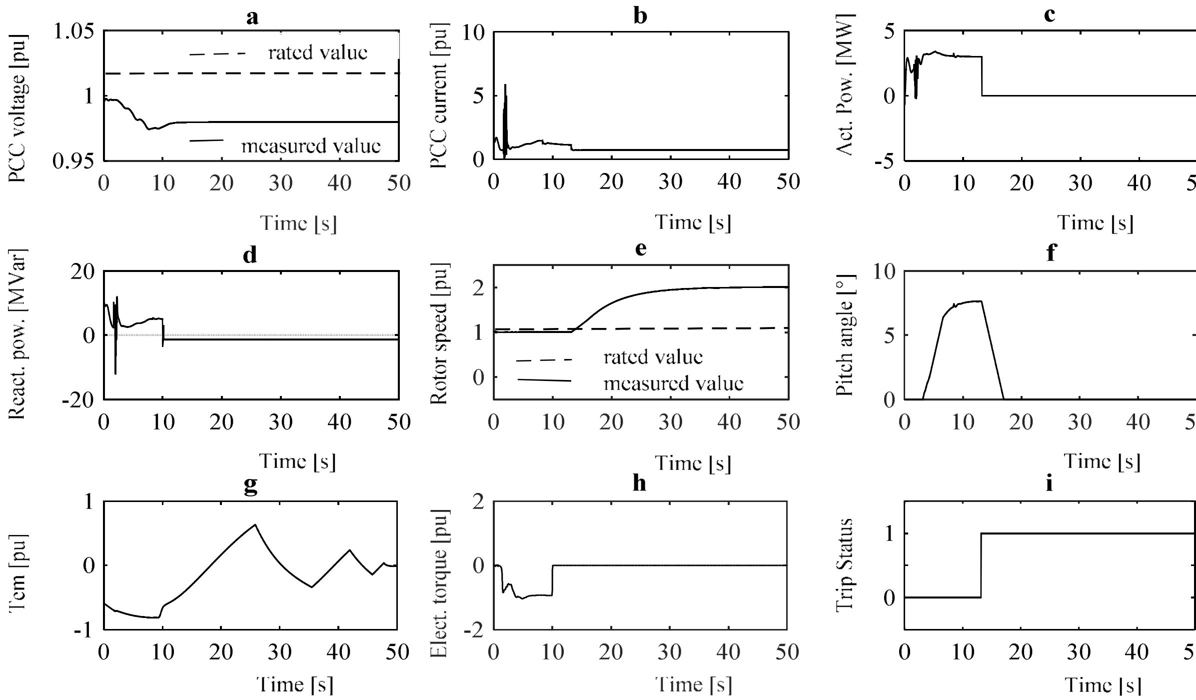

Fig. 13: Response of wind farm equipped with SCIG without compensation

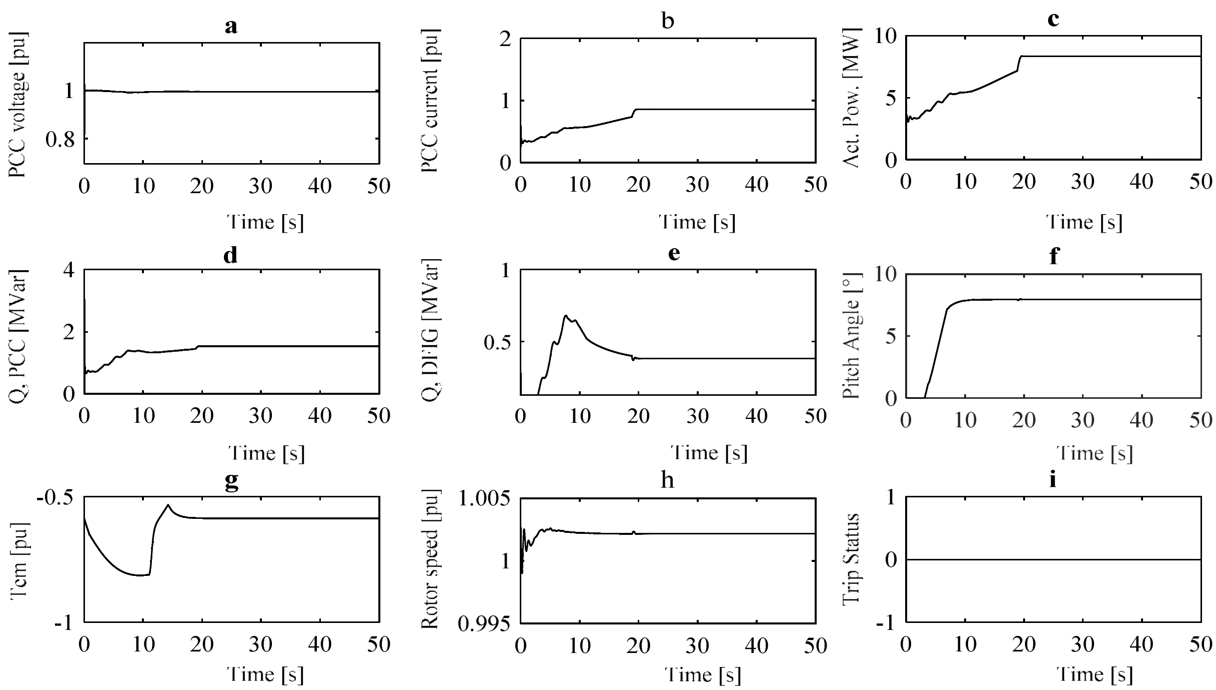

Fig. 14: Response of the system equipped with involving DFIG-WF

This low voltage leads to acceleration of the rotor speed of the generator and the torque cannot be maintained at its nominal value and several peaks appear which can affect the mechanical parts of the system and reduce the life time of the machine if no countermeasures are taken (Fig. 13e and 13g). Furthermore, this low voltage leads to an overall instability and the SCIG-WF disconnected from the grid at t = 15s via a system protection as shown in (Fig. 13i).

However, this behaviour is not accepted any more by the recent grid code which requires the wind turbines to remain online when the fault occurs in the system in order fulfilling the LVRT capability.

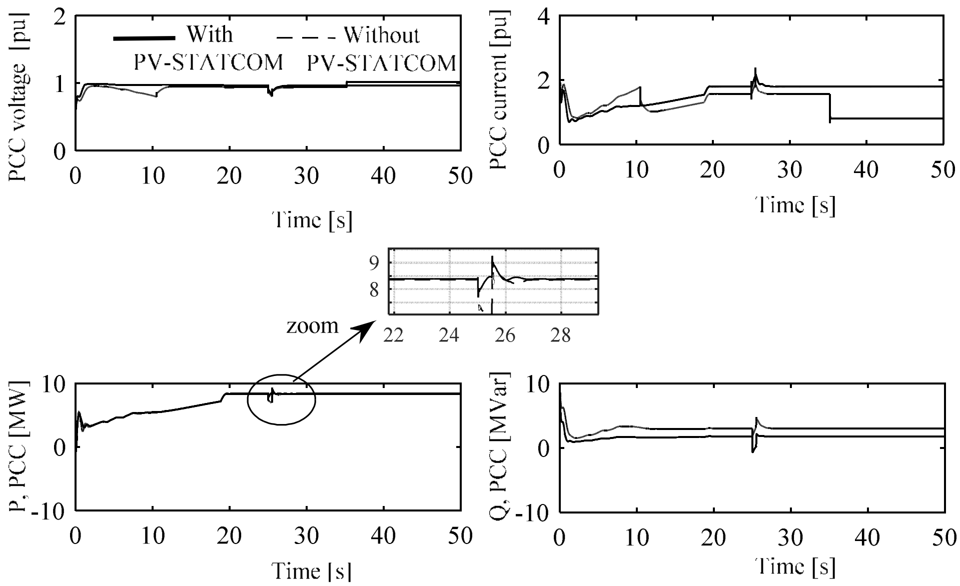

Fig. 15: Response of the system during grid fault with and without PV-STATCOM

In the second case study, the DFIG wind farm is involved in the system. The results are shown in Fig. 14. In this case, the grid side converter of the DFIG is designed to control the voltage and the active and the reactive power at the PCC of the system.

As we can observe, the PCC voltage is now regulated and maintained at 0.995 p.u. by generating 0.38 MVar (Fig. 14a to 14e).

The oscillations in the torque are reduced and the rotor speed does not exceed its rated value (Fig. 14g and 14h) and the system continued its operation without tripping from the grid which clarify that the system's performances are enhanced. The obtained results are similar to which presented in Wessels *et al*. (2013) and Obando-Montaño *et al*. (2014) whose used the STATCOM to ensure system stability but here in our work the main difference between the mentioned works is the use of the GSC of the DFIG to achieve the same purpose (Fig. 14).

The system response under grid fault with and without the PV-STATCOM is shown in Fig. 15.

The fault is presented by a dip voltage in the grid (three phase amplitude drops to 20%), the fault occurs at t = 25 s to 25.5 s.

As we can see, the fault is not self-clearing and the PCC voltage drops to 0.8 p.u. and the GSC of the DFIG cannot supply enough reactive power required by the system because of its small power capacity typically about 25% to 30% of the total power rating. This can lead to system instability as we were seen in the first situation (Fig. 13). Therefore, the wind farm should be immediately removed from the grid in order to prevent the overload issue.

Whereas, when the PV-STATCOM is connected to the PCC, the voltage is compensated and the transient stability of the system is improved which would have otherwise required expensive additional devices to accomplish the same objective, such as SVC or STATCOM as presented and discussed in Wessels *et al*. (2013) and Luo *et al*. (2016). Thus, we can conclude that the proposed control for PV-SPC to operate as a shunt compensator is demonstrated.

CONCLUSION

The novel contribution of this study is to use the DFIG wind farm and PV-STATCOM to improve the performances of the Point Common Coupling (PCC) of the existing SCIG wind farm. The reactive power required by the SCIG-wind farm can be supplied either by the DFIG-WF (during normal condition) and with the PV-STATCOM during grid disturbances. Under the obtained results, we can conclude that the performances and the efficiency of the proposed system are improved by the proposed control system.

This new concept has a low cost compared to the conventional expensive devices which they used to accomplish the same objective, such as SVC and STATCOM. As well as, is 100% renewable energy and can lead to encouraging the potential integration of wind farm in the future.

REFERENCES

Abad, G., J. Lopez, M. Rodriguez, L. Marroyo and G. Iwanski, 2011. Doubly Fed Induction Machine: Modeling and Control for Wind Energy Generation Applications. Wiley, Hoboken, N.J.

Aziz, T., T.K. Saha and N. Mithulananthan, 2014. A Review of Interconnection Rules for Large-scale Renewable Power Generation. In: Hossain, J. and

A. Mahmud (Eds.), Large Scale Renewable Power Generation, Advances in Technologies for Generation, Transmission and Storage. Springer, Singapore, pp: 151-171.

Baggu, M.M., 2009. Advanced control techniques for doubly fed induction generator-based wind turbine converters to improve low voltage ride-through during system imbalances. Ph.D. Thesis, Missouri University of Science and Technology.

Bhaskar, M.A., S.S. Dash, R. Magdal, J. Jerry, A. Mohammed Tamheed, S. Laksshman and S. Aravindan, 2012. Application of integrated wind energy conversion system (WECS) and photovoltaic (PV) solar farm as STATCOM to regulate grid voltage during night time. Energ. Proc., 14: 1536-1541.

Bhatti, A.R., Z. Salam, M.J.B. Abdul Aziz and K.P. Yee, 2015. A critical review of electric vehicle charging using solar photovoltaic. Int. J. Energ. Res., 40(4): 439-461.

Blaabjerg, F. and K. Ma, 2014. High Power Electronics: Key Technology for Wind Turbines. In: Abu-Rub, H., M. Malinowski and K. Al Haddad (Eds.), Power Electronics for Renewable Energy Systems, Transportation and Industrial Applications. IEEE Press and John Wiley and Sons Ltd., pp: 140-141.

Cardenas, R., R. Pena, S. Alepuz and G. Asher, 2013. Overview of control systems for the operation of DFIGs in wind energy applications. IEEE T. Ind. Electron., 60(7): 2776-2798.

Chakraborty, S., M.G. Simões and W.E. Kramer, 2013. Power electronics for renewable and distributed energy Systems: A Sourcebook of Topologies, Control and Integration. Springer, London, New York.

Duong, M.Q., F. Grimaccia, S. Leva, M. Mussetta and K.H. Le, 2015. Improving transient stability in a grid-connected squirrel-cage induction generator wind turbine system using a fuzzy logic controllers. Energies, 8(7): 6328-6349.

Farret, F.A., M.G. Simões and A. Michels, 2014. Small Hydroelectric Systems. In: Chakraborty, S., M.G. Simões and W.E. Kramer (Eds.), Power Electronics for Renewable and Distributed Energy Systems. Springer, London Heidelberg, New York, pp: 170-175.

Grigsby, L.L., 2012. The Electric Power Engineering Handbook. 3rd Edn., Taylor & Francis, CRC, Boca Raton, Fla., London, New York.

Gupta, A., S. Chanana and T. Thakur, 2014. THD reduction with reactive power compensation for fuzzy logic DVR based solar PV grid connected system. Front. Energ., 8(4): 464- 479.

Luo, A., Q. Xu, F. Ma and Y. Chen, 2016. Overview of power quality analysis and control technology for the smart grid. J. Mod. Power Syst. Clean Energ., 4(1): 1-9.

Malek, H., 2014. Control of grid-connected photovoltaic systems using fractional order operators. Ph.D. Thesis, Utah State University, Logan, Utah.

Muthuramalingam, M. and P.S. Manoharan, 2014. Simulation and experimental verification of intelligence MPPT algorithms for standalone photovoltaic systems. Res. J. Appl. Sci. Eng. Technol., 8(14): 1695-1704.

Obando-Montaño, A.F., C. Carrillo, J. Cidrás and E. Díaz-Dorado, 2014. A STATCOM with supercapacitors for low-voltage ride-through in fixed-speed wind turbines. Energies, 7(9): 5922-5952.

Padiyar, K.R., 2007. FACTS Controllers in Power Transmission and Distribution Solar. New Age International, India.

Qiao, W., 2012. Power Electronics for Renewable Energy. In: Grigsby, L.L. (Ed.), the Electric Power Engineering Handbook. 3rd Edn., Taylor & Francis Group, London, New York, pp: 535-536.

Sankarganesh, R. and S. Thangavel, 2014. Performance analysis of various DC-DC converters with optimum controllers for PV applications. Res. J. Appl. Sci. Eng. Technol., 8(8): 929-941.

Sen, K.K. and M.L. Sen, 2009. Introduction to FACTS Controllers: Theory, Modeling, and Applications. John Wiley & Sons, IEEE Press, Piscataway, Hoboken, New Jersey.

Shao, S., T. Long, E. Abdi and R.A. McMahon, 2013. Dynamic control of the brushless doubly fed induction generator under unbalanced operation. IEEE T. Ind. Electron., 60(6): 2465-2476.

Sumathi, S., L. Ashok Kumar and P. Surekha, 2015. Solar PV and Wind Energy Conversion Systems: An Introduction to Theory, Modeling with MATLAB/SIMULINK, and the Role of Soft Computing Techniques. Springer, Cham, New York.

Suul, J.A., M. Molinas and T. Undeland, 2010. STATCOM-based indirect torque control of induction machines during voltage recovery after grid faults. IEEE T. Power Electr., 25(5): 1240-1250.

Tan, K.H., 2016. Squirrel-cage induction generator system using wavelet petri fuzzy neural network control for wind power applications. IEEE T. Power Electr., 31(7): 5242-5254.

Varma, R.K., S. Arifur Rahman and T. Vanderheide, 2015. New control of PV solar farm as STATCOM (PV-STATCOM) for increasing grid power transmission limits during night and day. IEEE T. Power Deliver., 30(2): 755-763.

Wessels, C., N. Hoffmann, M. Molinas and F. Wilhelm Fuchs, 2013. StatCom control at wind farms with fixed-speed induction generators under asymmetrical grid faults. IEEE T. Ind. Electron., 60(7): 2864-2873.

Xu, L., L. Yao and C. Sasse, 2006. Comparison of using SVC and STATCOM for wind farm integration. Proceeding of the International Conference on Power System Technology, Chongqing, Oct. 22-26, pp: 1-7.

Yao, J., H. Li, Z. Chen, X. Xia, X. Chen, Q. Li and Y. Liao, 2013. Enhanced control of a DFIG-based wind-power generation system with series grid-side converter under unbalanced grid voltage conditions. IEEE T. Power Electr., 28(7): 3167-3181.

Zou, Y., M. Elbuluk and Y. Sozer, 2013. Simulation comparisons and implementation of induction generator wind power systems. IEEE T. Ind. Appl., 49(3): 1119-1128.